

# Integrated Analysis of Surface and Borehole Data to Construct the Stratigraphy Model of Bukit Daun Field, Indonesia

Muhammad Ikhwan<sup>1</sup>, Irene C Wallis<sup>2</sup> and Julie V Rowland<sup>2</sup>

<sup>1</sup> Pertamina Geothermal Energy, Skyline Building Level 19<sup>th</sup>, Jalan M. H. Thamrin No.9, Jakarta, Indonesia

<sup>2</sup> School of Environment, University of Auckland, 23 Symond Street, Auckland Central, New Zealand

ikhwan.aziz@pertamina.com

**Keywords:** Bukit Daun, Sumatra, geological model, permeability, hydrology, geothermal system, exploration

## ABSTRACT

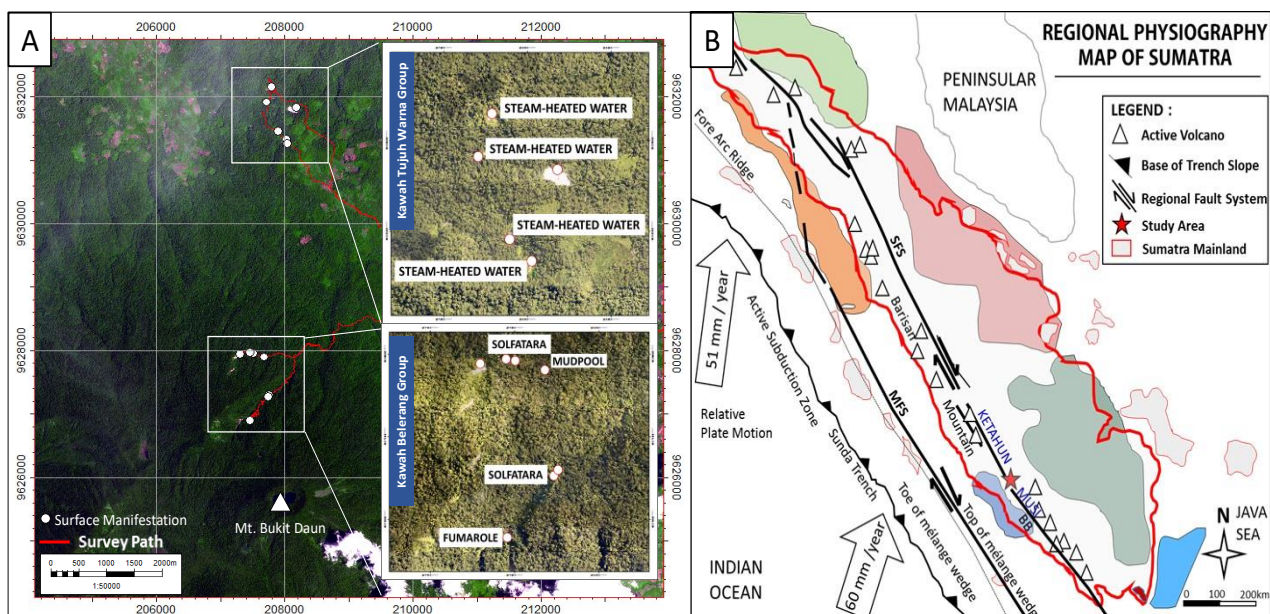
We present the results of detail stratigraphic identification of the Bukit Daun geothermal field, Indonesia. This study optimizes the available surface and subsurface data to comprehensively reveal the lithology condition of the field with the regional data that is visualized in the 2D and 3D stratigraphic models.

The extensive use of the image log analysis has improved the geologic interpretation's confidence, which combines with terrain imagery analysis and drilling parameters and data such as cutting and core. The metasedimentary deposit that contains fossil enables us to predict the formation age of the reservoir rocks. The well test result also supports the geologic influence in permeability.

## 1. INTRODUCTION

Bukit Daun field is administratively located in Bengkulu province, about 60 km to the northeast of Bengkulu's capital city in the southern part of Sumatra. It is owned and operated by PT. Pertamina Geothermal Energy. Bukit Daun is a geothermal prospect that occurs in association with volcanic centers and the Sumatra Fault System (SFS). It lies between the tips of two adjacent fault segments: the Musi and Ketahun segments (Figure 1.B). Topography images show a clear separation of these segments, but the structural architecture could not be described as an overlapping right-stepover (Sieh & Natawidjaja, 2000). The Musi and Ketahun segments may link to the northwest, but young volcanic deposits obscure the fault structure. The zone between the segment tips is co-extant with a Holocene volcanic field.

The geothermal resource in the Bukit Daun field is indicated by the presence of surface manifestations including fumaroles, solfatara, mudpools, and steam-heated water that discharges in the flank of the volcanic centre and ~3 km to the north, in the northern part of the Bukit Daun volcanic area (Figure 1.A). PT. Pertamina Geothermal Energy (PGE) drilled three exploration wells at Bukit Daun in 2016 that intersected a viable high-temperature geothermal resource with benign fluids. In this paper, we present the process and results from a study that combines data from that drilling campaign with publicly available data to generate a geologic model of Bukit Daun and consider geologic controls on fluid flow at the well- and reservoir-scale (Ikhwan, 2020). We will describe our interpretation of the stratigraphic and structural setting that was used to generate a 3D geologic model.



**Figure 1: A) Distribution of thermal manifestations at Bukit Daun field. B) Bukit Daun field plotted with key geologic-physiographic features in Sumatra (after Moore and Curray, 1980; Darman and Sidi, 2000) where BB = Bengkulu Basin, SFS = Sumatra Fault System, and MFS = Mentawai Fault System.**

## 2. REGIONAL GEOLOGY

Tectonically, three major crustal-to-lithospheric scale faults are recognised in Sumatra (Figure 1.B). First, the Sunda Trench marks the trace of the subduction thrust interface between the Eurasian and Indian Ocean plates. Convergence is highly oblique with the strike-slip component of plate motion transferred into the overriding plate. Second, the right-lateral strike-slip Sumatra Fault System (SFS) accommodates up to 6 mm/yr of the oblique convergence (Bellier & Sébrier, 1994). The shape of this fault is sinuous, and it extends from Banda Aceh in the north to Lampung in the south. Third, the Mentawai Fault System (MFS) occurs in the forearc and also accommodates a component of strike-slip, although its kinematics may be complex (Darman & Sidi, 2000).

Much of the regional and local Bukit Daun geological setting also described in Ikhwan et al. (2020), which discuss the comprehensive geology and permeability control, and Ikhwan (2020), which discuss the detailed structural framework within the regional and local area of Bukit Daun. Due to its location between the Bengkulu Basin and the Barisan Mountains, the Bukit Daun geothermal system's stratigraphy is influenced by both sedimentary and volcanic deposits. Drilling and surface mapping has confirmed Neogene-Paleogene metasedimentary deposits, which are interlayered with and overlain by Quaternary lava and pyroclastic products. The Bukit Daun field is dominated by the presence of a stratovolcanic centre with geomorphic evidence for multiple eruptive vents and flows. Much of the area is covered by Quaternary volcanic products, and these blanket the geothermal field.

## 3. STRATIGRAPHY

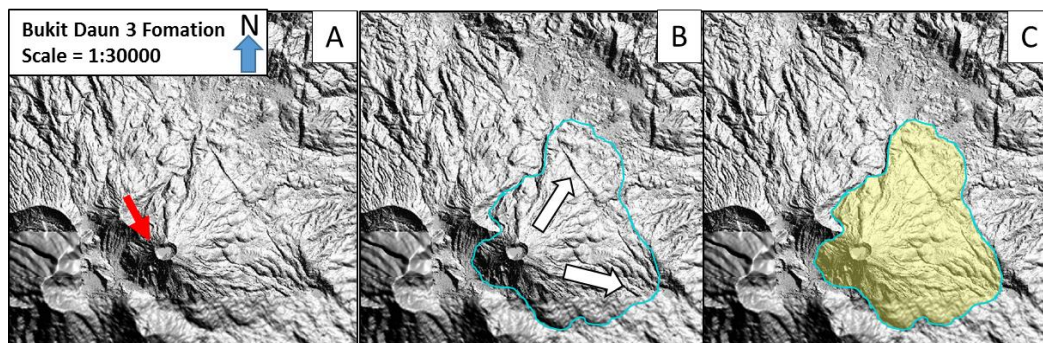
The study area is dominated by the presence of a stratovolcanic centre with geomorphic evidence for multiple eruptive vents and flows. Much of the area is covered by Quaternary volcanic products, and these blanket the thermal area. In this paper, we define a stratigraphic framework for the Bukit Daun geothermal system based on geomorphic and subsurface evidence for distinct mappable units placed in the regional geology context. Cuttings, core, borehole logs, and fossil data are the primary tools for the recognition of the formation boundaries that are used in the construction of the 3D geological model.

### 3.1 Surface Stratigraphy

LiDAR, in combination with an IFSAR (DEM) image, is used to construct the geological map over a 25 km<sup>2</sup> area that includes the geothermal field. Construction includes amendments to formation boundaries and their distribution. An understanding of regional geology, tectonic and volcanic geomorphology, and image interpretation underpin these constructions. No new field mapping was undertaken to ground-truth the revised map because the expense was deemed unlikely to yield sufficient reward given the access difficulties and lack of outcrop due to jungle cover and intense weathering profiles. However, this study is also supported by the field data conducted by PGE on the previous work.

The imagery available for this study is grayscale. Rock units and their contacts (lithological, structural) are delineated by their geomorphic expression, contrast, and reflectance (Hou & Wei, 2002). The imagery was analysed using standard tools within ArcGIS® software. The basic settings of image analysis imagery are: 1) Hillshade display (grayscale 3D representation of the surface) provided in ArcGIS tools. 2) The lighting (sun) angle is 45° (from NE to SW), perpendicular to the structural trend (SFS). 3) The scale of the image is 1:79000

As a stratovolcano area, the field study's geomorphological interpretation refers to associated volcanic landform and lava flow features, which are used as the basis of formation boundary delineations. Such features seen and analysed on the images are eruption vents, lava lobes, levees, radial patterns, concentrated-flow, and ash plateaus. Drainage patterns provide additional constraints. For instance, Figure 2 shows the interpretation of a formation boundaries delineation. A blank topographic map (IFSAR + LiDAR) is depicted on the left. The formation boundary's delineation is shown at centre, and the interpreted formation is shown on the right.



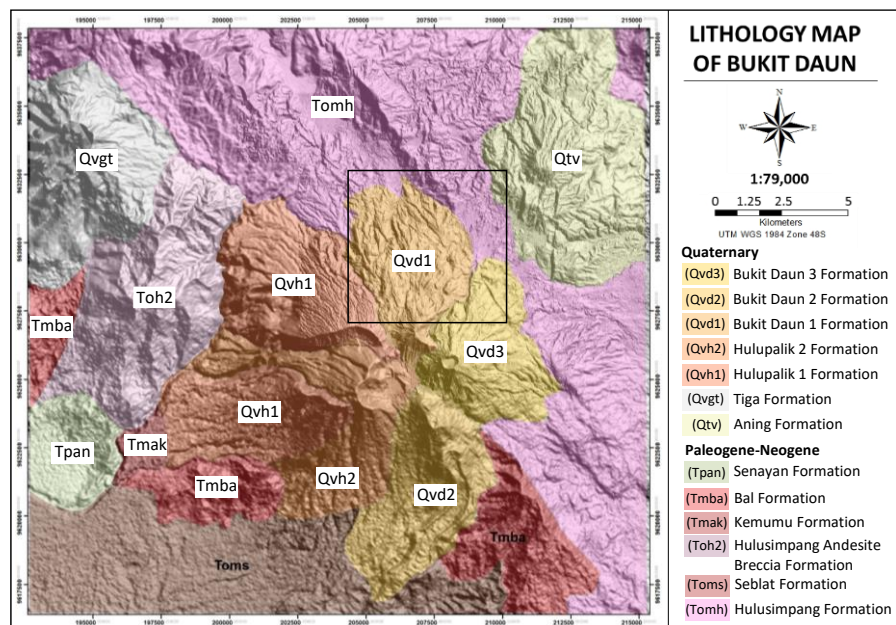
**Figure 2: Delineation of Bukit Daun 3 formation. A) The eruption centre of the Bukit Daun 3 formation is clearly visible in the topographic image. A circular caldera feature marks the top of this formation. The red arrow shows the eruption centre. B) The lava levees show that the lava flows are more developed and directed relatively to NE and E. Some of the lava lobes are also directed in this direction. An NW-SE structure blocks this lava flow and acts as the boundary of this formation in the lower east part. C) Coloured Bukit Daun 3 formation.**

The following observations can be drawn from the revised map and available data (PGE unpublished report, 2015):

1. The oldest mapped Pre-Quaternary volcanic product is the Hulusimpang (Tomh) Formation and dominates the study area. Hulusimpang Formation mostly consists of tuff and pyroclastic deposits but also includes as andesite lava and andesite breccia (Toh2) in the west part of Mt. Bukit Daun. In the southern region, another deposit (Seblat Formation, Toms) is exposed. It's known that this formation has an inter-fingering relationship with Hulusim-pang Formation (Gafoer et al., 1992). Both formations were emplaced or deposited in the late Oligocene to early Miocene.



2. Neogene andesite and andesitic breccias occur in the southwestern quarter of the study area and overlie the older Formations. These units are mapped as Kemumu (Tmak) and Senayan (Tpan) Formations. The eruption centre for these units is unclear; erosion during the Pliocene-to-Pleistocene orogenic phase destroyed diagnostic geomorphic features.
3. A Neogene dacitic epiclastic formation appears in the western and southern part of Bukit Daun and is called Bal formation (Tmba). This formation overlies Hulusimpang and Seblat formations and was deposited during the middle to late Miocene.
4. The Hulupalik and Bukit Daun Formations are the youngest Quaternary deposits. Hulupalik formation appears to have a greater volume than Bukit Daun formation. The eruptive products of the Hulupalik formation are divided into two phases, Hulupalik 1 and Hulupalik 2, based on the presence of pyrite in the latter deposit (PGE unpublished report, 2015). These formations dominantly erupted to the west side of the Hulupalik volcanic centre.
5. Volcanic products of the Bukit Daun Formation are divided into three phases based on their eruption sequence and physical composition. Bukit Daun 1 formation is the first volcanic product of Bukit Daun and spread toward the north. Bukit Daun 2 results from the emplacement of volcanic products to the south of the main edifice. The last eruptive phase of Bukit Daun yielded the Bukit Daun 3 formation that spread mostly to the north and southeast. Bukit Daun 3 overlies Bukit Daun 1 in the north and part of Bukit Daun 2 in the south.



**Figure 3: Revised surface stratigraphic map of Bukit Daun field. Black box: the prospect area.**

### 3.2 Subsurface Stratigraphy

The locations of the three exploration wells used in this study to confirm the geothermal resource are shown in Figure 9.A. The wells are labeled according to the drilling date: Well-A, Well-B, and Well-C. Each well is deviated and designed as a big-hole casing.

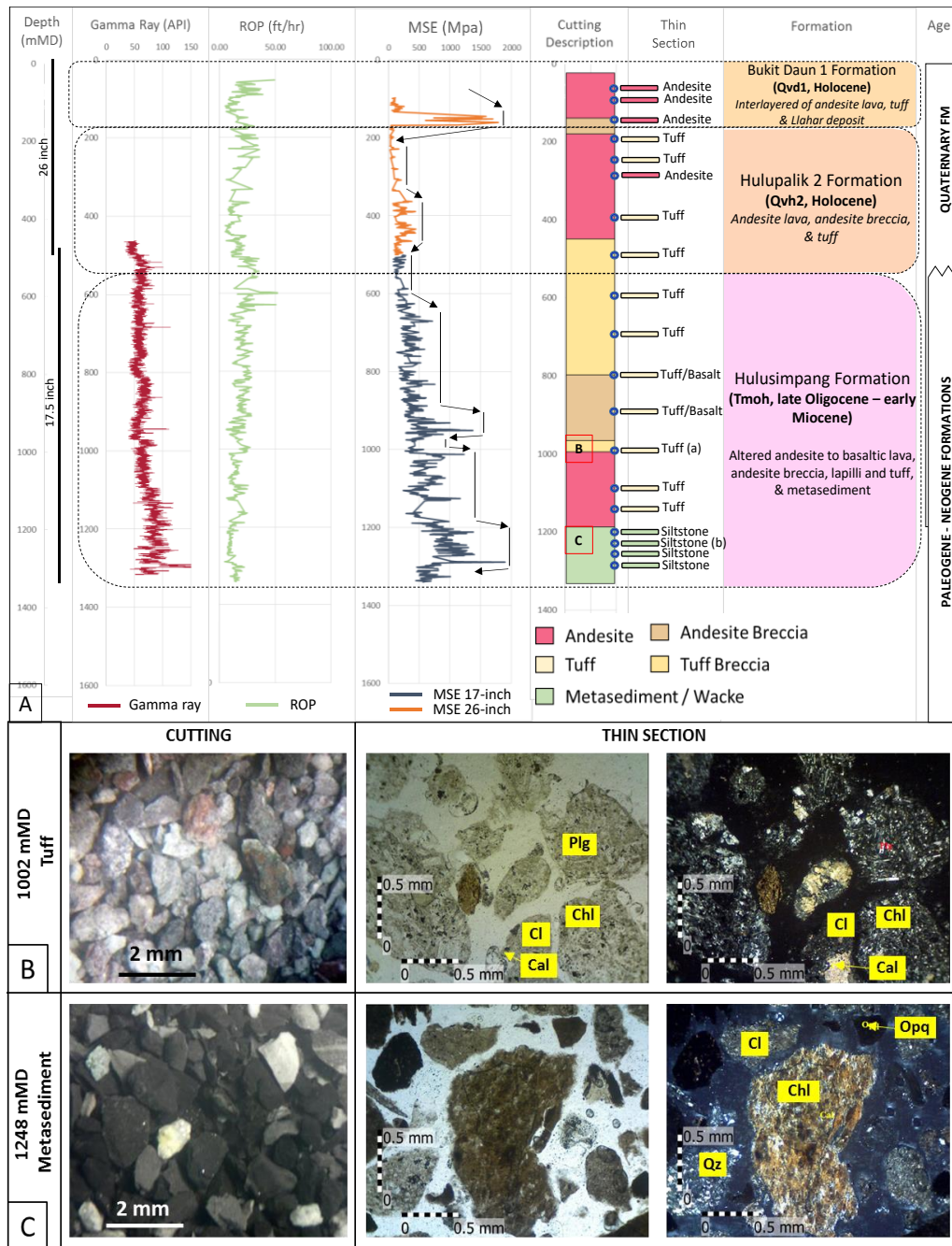
The identification of formation contacts in wells is vital to determine the subsurface stratigraphy. As the cutting, thin section, and core data have significant spatial uncertainty, the delineation of contacts relies on the borehole image and log data. Unfortunately, the borehole image is only available on the 12.25" and 9.875" holes (reservoir interval). Thus, drilling parameters (e.g., ROP/rate of penetration, RPM/rotation per minute, or torque which combined to calculate the formation mechanical specific energy) together with cutting data were used to identify the position of formation contacts for those intervals not covered by borehole imagery and logging data. The following sections present the borehole stratigraphy for each well inferred from the joint interpretation of such data and through integration with supplementary information (e.g., fossils) where available.

#### 3.2.1 Well-A

Well-A pad is situated in Bukit Daun 1 formation, one of the youngest units in the study area. The description of borehole stratigraphy together with supporting evidence, is illustrated in Figure 4 (interval without borehole imagery) and Figure 5 (interval with borehole imagery).

From the surface to the production casing point (1300 mMD), Well-A intersected Bukit Daun 1, Hulupalik 2, and Hulusimpang Formations. Hulupalik 1 Formation was presumably absent because it is focused on the west side of the Hulupalik volcanic centre (HVC). Bukit Daun 2 formation also is not present as it erupted to the south of HVC. The Hulupalik 2 formation unconformably overlies the Hulusimpang Formation. This contact is marked by an inflection in the MSE plot at 550 mMD. The dominance of tuff and volcanic breccia below this depth supports its interpretation as the top of the Hulusimpang Formation. Moreover, increases in signal magnitude on the gamma log and MSE data (noting that the increase in the latter is subdued because the well diameter increases at this depth) support the hardness contrast of Hulusimpang with the former formation. Thus, the unconformity between Quaternary and Neogene formations in Well-A is interpreted to coincide with this contact. This depth also corresponds with the orogenic erosion surface in the field study area. Gamma-ray dates were not recorded from the surface to 436 mMD.

From immediately below the production casing depth to 3000 mMD (the production zone interval), Well-A penetrates Hulusimpang, Kikim, and Saling formations (Figure 5). Kikim is the oldest Paleogene unit in the study area and is dominated by welded tuff. It unconformably overlies the Cretaceous Saling formation at 2450 mMD. It consists of lava and tuff, primarily, and is characterized by the presence of abundant epidote and chlorite, which can be seen in the cutting and core samples. A diorite intrusion has been identified in a conventional core sample, and it intrudes the Kikim formation at 2170 mMD. Unfortunately, the thickness of the diorite is unclear since the core sample is not representative in terms of length and recovery (3-metre sample from 5.5-metre coring length). The diorite is yet to be dated but is likely to be Miocene based on its regional context (Gafoer et al., 1992).



**Figure 4: Stratigraphy of Well-A from the surface to 1300 mMD (no borehole image interval) derived from cutting and thin section description (PGE unpublished report, 2015), gamma-ray log, ROP, and MSE. The formation colours are coded to the lithological map. The red box with letter inside is the location of the cutting and thin section shown in the lower figure. B & C) Cutting and thin section samples of tuff and metasediment. Mineral symbol: Plg=Plagioclase, Chl=Chloride, Cl=Clay, Cal=Calcite, Qz=Quartz, Opq=Opaque**



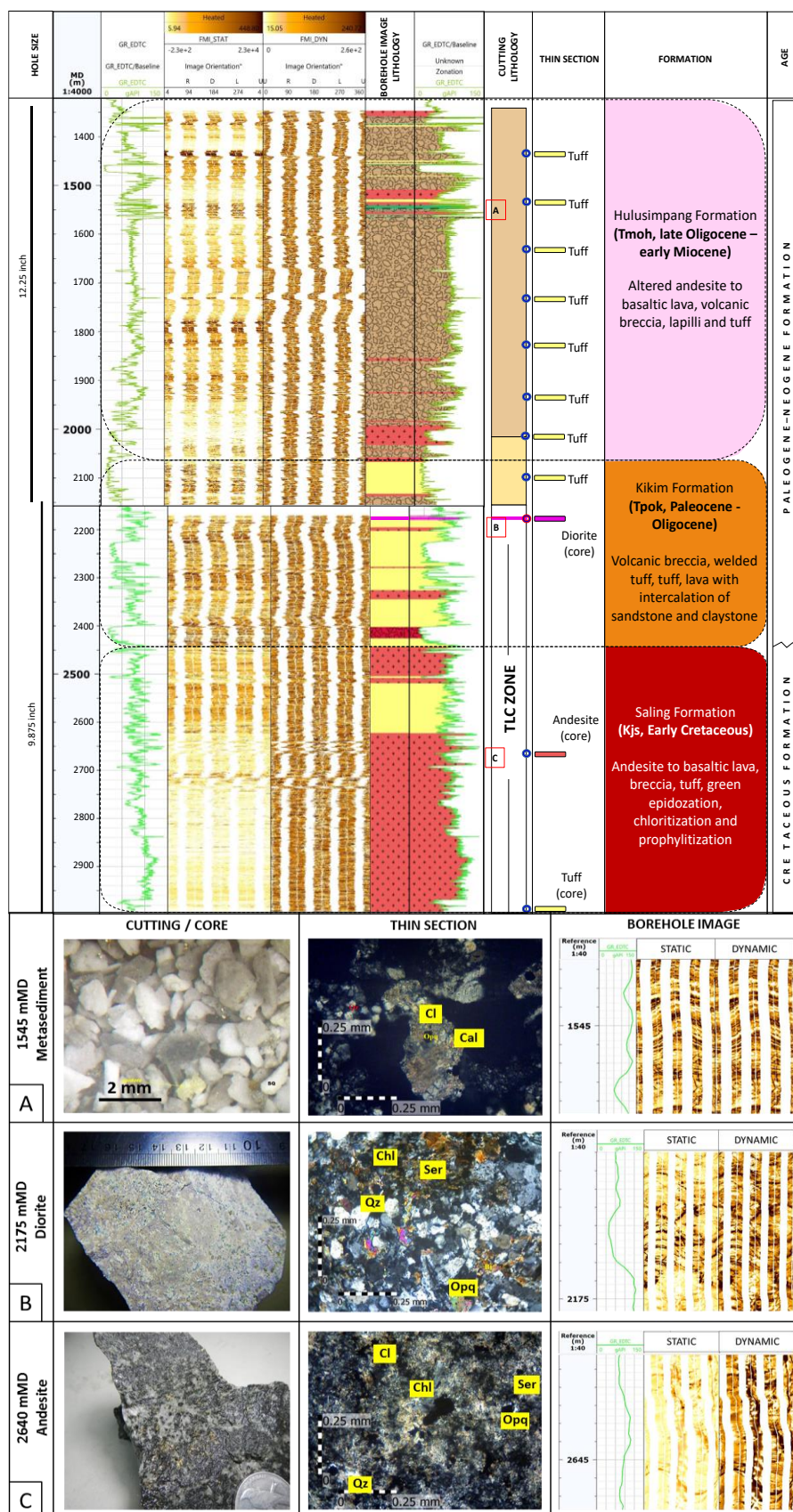


Figure 5: (Upper) Stratigraphy of Well-A from 1300 to TD (borehole image interval) derived from cutting, core, and thin section description (PGE unpublished report, 2015), borehole image, and gamma-ray log. The formation colours are coded to the lithological map. The red box with letter inside is the location of the cutting and thin section showed in Figure 4.14. TLC = Total Loss Circulation. (Lower) A presentation of cutting/core sample, thin section, and image logs from selected depth in Well-A. A) Metasediment cutting sample. B) Diorite conventional core sample. C) Andesite conventional core sample. Mineral symbol: Plg=Plagioclase, Chl=Chloride, Cl=Clay, Cal=Calcite, Qz=Quartz, Opq=Opaque, Ser=Sericite.

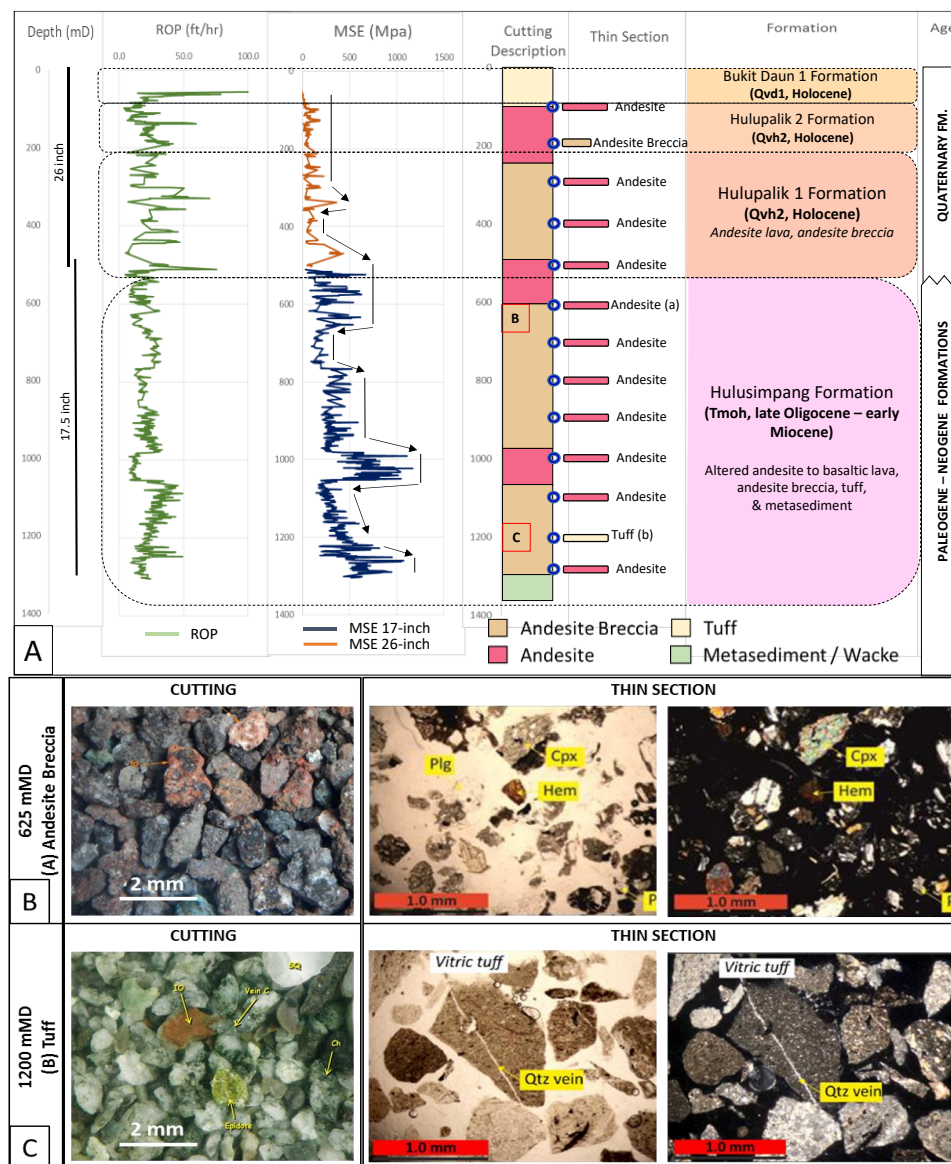
### 3.2.2 Well-B

Well-B was drilled adjacent to Well-A. Thus the stratigraphy is much similar (Figure 6, interpreted without borehole imagery; Figure 7 interpreted with borehole imagery).

From the surface until the production casing point interval, Well-B penetrates Bukit Daun 1, Hulupalik 2, Hulupalik 1, and Hulusimpang formation (Figure 6). The contact between Hulupalik 1 with Hulusimpang formation is marked by a change in the ROP and MSE signals at 545 mMD corresponding with the Quaternary-Neogene erosional unconformity. Compared with Well-A, this contact is at relatively the same elevation. However, in contrast to Well-A, tuff is not dominant; instead, andesite and breccia are abundant. No gamma-ray log was recorded in this interval.

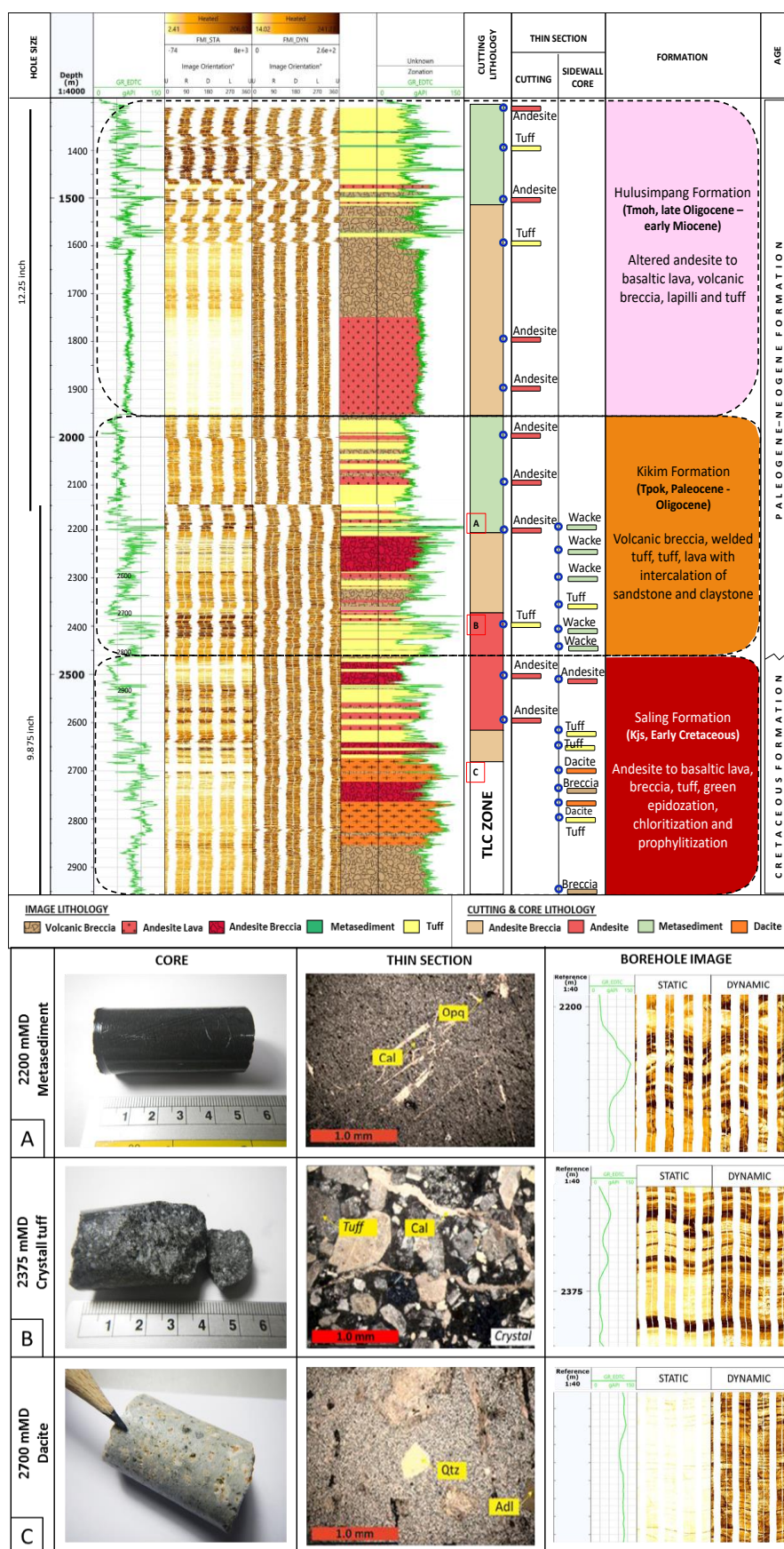
From the production casing point (1300 mMD) to TD, Well-B consists of Paleo-Neogene and Cretaceous formations (Figure 7). Hulusimpang formation overlies the Kikim formation, and the contact between Kikim and Saling formations at 2460 mMD represents the Paleogene - Cretaceous boundary. In Well-B, Saling formation consists of a more diverse range of lithologies. Dacitic products dominate in some intervals and are interlayered with breccia, lava, and tuff. The diorite intrusion is absent.

Within this deeper interval, three cutting samples containing abundant fossils within metasedimentary material were found at 1501, 2002, and 2101 mMD. Fossils analysis was conducted by the PGE team (PGE unpublished report, 2015). Three foraminifera species were recognised based on characteristics defined by Bolli & Saunders (1985) and Postuma (1971): *Globigerinoides primordius* (late Oligocene to early Miocene) in Hulusimpang formation, *Globigerina praebulloides praebulloides* (late Eocene to middle Miocene) in Kikim formation, and *Globigerina ciperoensis ciperoensis* (middle Oligocene) in Kikim formation. Each species indicates an age range that matches the suggested formation age where they were found.



**Figure 6: Stratigraphy of Well-A from 1300 to TD (borehole image interval) derived from cutting, core, and thin section description (PGE unpublished report, 2015), borehole image, and gamma-ray log. The formation colours are coded to the lithological map. The red box with letter inside is the location of the cutting and thin section showed in Figure 4.14. TLC = Total Loss Circulation.**

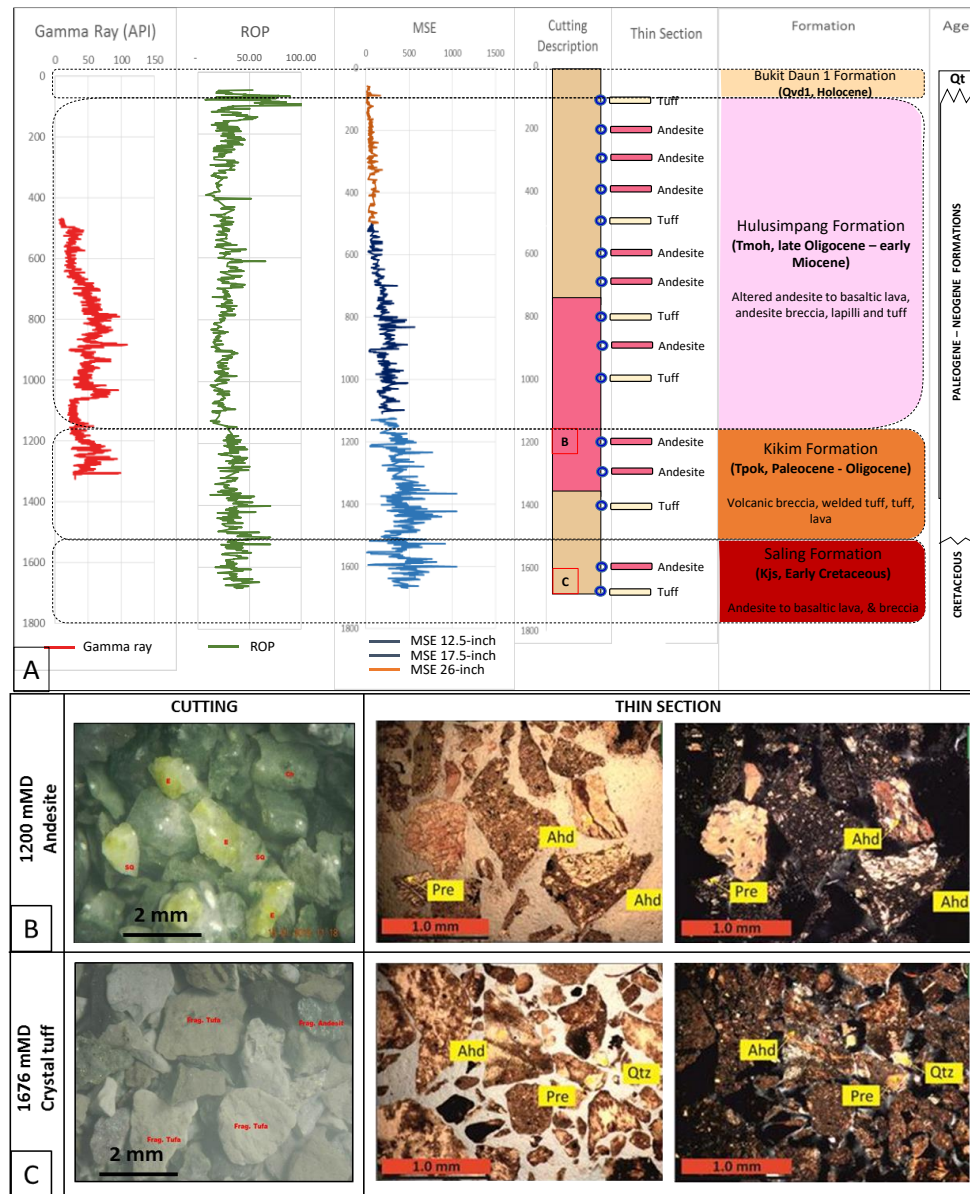




**Figure 7: (Upper) Stratigraphy of Well-B from 1300 to TD (borehole image interval) derived from cutting, core, and thin section description (PGE unpublished report, 2015), borehole image, and gamma-ray log. The formation colours are coded to the lithological map. The red box with letter inside is the location of the cutting and thin section showed in Figure 4.17. TLC = Total Loss Circulation. (Lower) A presentation of cutting/core samples, thin section, and image logs from selected depth in Well-B. A) Metasediment sidewall core sample. B) Crystalline sidewall core sample. C) Dacite sidewall core sample. Mineral symbol: Cal=Calcite, Qz=Quartz, Opq=Opaque, Adl=Adularia.**

### 3.2.3 Well-C

Well-C has sited on Bukit Daun 1 formation, which is dominated by tuff and volcanic breccia. This formation overlies the Hulusimpang formation as inferred from field relationships: the Hulusimpang formation is exposed to the northern part of the well pad. Thus, the well intersects the Quaternary-Neogene erosional unconformity at shallow depth. Because the basement rocks are uplifted in the study area, Well-C was expected to penetrate the Kikim and Saling formations. The inferred stratigraphy based on joint interpretation of subsurface data and field relationships is shown in Figure 8.



**Figure 8:** A) Stratigraphy of Well-C from surface to 1658 mMD (no borehole image interval) derived from cutting and thin section description (PGE unpublished report, 2015), gamma-ray, ROP, and MSE. The formation colours are coded to the lithological map. The red box with letter inside is the location of the cutting and thin section showed in lower figures. B & C) Cutting and thin section samples of andesite and crystal tuff. Minerals symbol: Pre=Prehnite, Ahd=Anhydrite, Qz=Quartz.

### 3.3 Stratigraphic Framework

Based on the borehole stratigraphy presented above and supported by surface and regional data, the stratigraphy of the Bukit Daun field can be summarised as follows:

1. The oldest formation penetrated by the wells is the Cretaceous basement rock, the Saling Formation (Kjs). This formation consists of lava, breccia, tuff, and dacite. The Saling formation was folded and uplifted during the late Cretaceous, rifted in association with subsequent basin development, and up-lifted again in response to the current subduction regime (McCarthy & Elders, 2014). The basement's tilting is toward the SW (Gafoer et al., 1992), consistent with the shallowing of this formation in the Well-C area.
2. Kikim Formation is dominated by welded tuffs which were deposited during the Eocene to early Oligocene (Barber et al., 2005). Sedimentary material in this formation records the development of rift basins in what Barber et al. (2005) refer to as the horst-and-graben stage. Miocene dioritic intrusions cross-cut this formation.

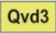
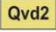


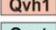
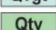


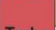
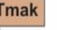

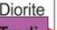
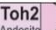

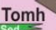
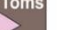
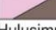
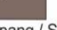


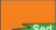





3. Hulusimpang Formation (Tomh) was deposited during the late Oligocene to early Miocene (Gafoer et al., 1992). It is characterized by various volcanic products including andesite lava, volcanic breccia, lahar deposit, tuffs, lapilli, metasedimentary units, and rare dacite. Metasedimentary units intersected by drilling indicate that this formation is deposited during an active sedimentation process in a transgressive environment (Kusnama et al. 1992). Hulusimpang formation is the latest Paleogene-Neogene formation identified from drilling, although some younger Neogene deposits are described on the surface.

4. Quaternary Hulupalik Formation (Qvh) is characterized by the andesite lava and andesitic breccias and is divided into Hulupalik 1 and Hulupalik 2, based on the presence of pyrite, mapped during company fieldwork (PGE unpublished report, 2015) and apparent in thin section analysis of borehole samples. However, generally, Hulupalik 1 and 2 cannot be distinguished on this basis.

5. The youngest formation recorded from subsurface data is Quaternary Bukit Daun Formation (Qvd). It is divided into three units based on the surface mapping. Mostly these consist of andesite lava, andesitic breccia, andesitic boulders, tuff, and volcanic breccia (Gafoer et al., 1992).

**Table 1: Bukit Daun field stratigraphic column, based on mapped and described subsurface formation, and modified after Gafoer et al. (1992) by adding the regional tectonic and stratigraphic stages and fault mechanism.**

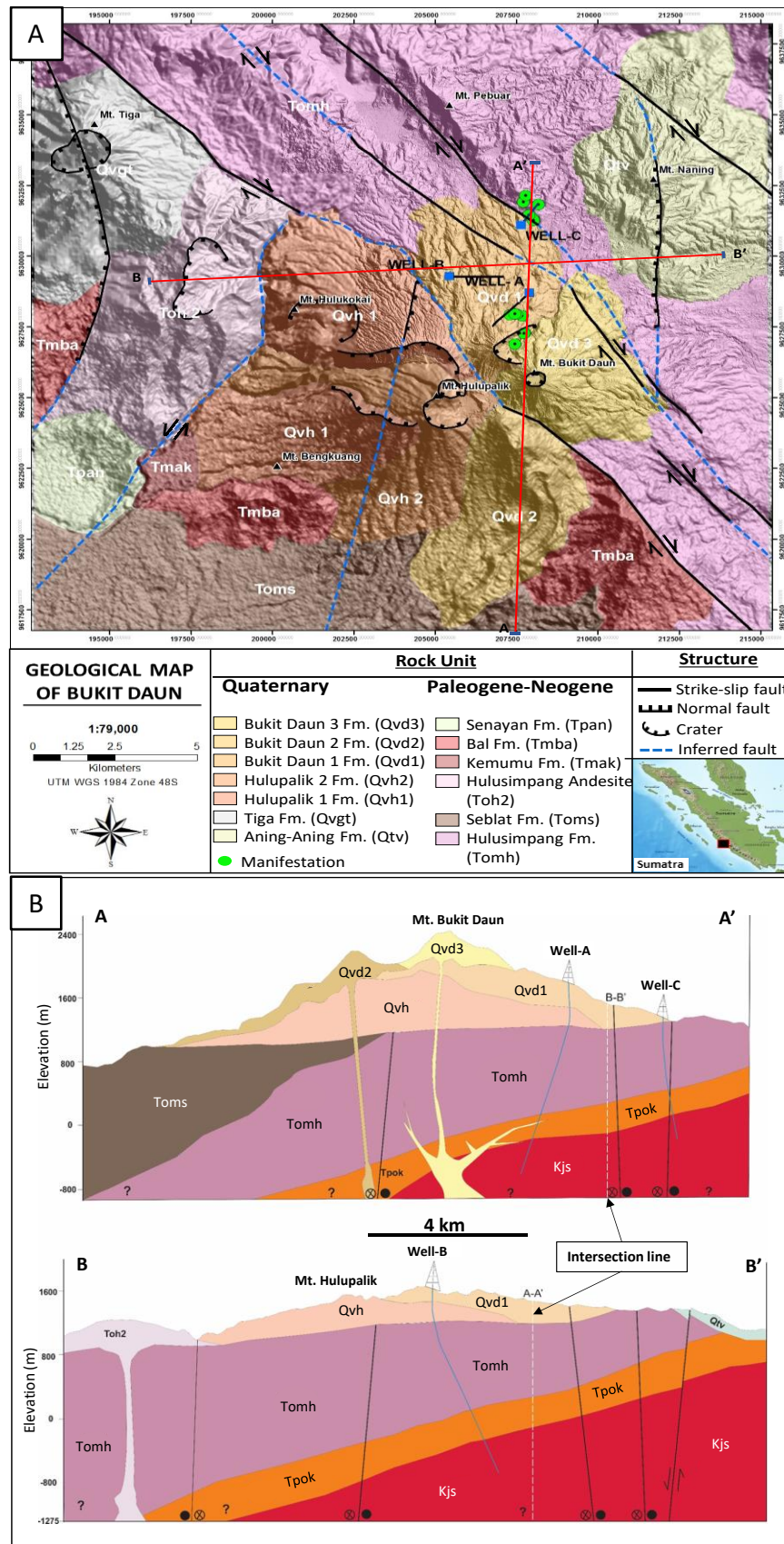
Reference Ages			Regional Tectonic and Stratigraphic Stages	Volcanic/Intrusion Product	Lithology	Fault Mechanism					
Quaternary <1.8 Ma			Renewed subduction along Sumatra trench resulted continues active volcanism  Reactivation - Continuity active Sumatra Fault	 Bukit Daun 3	Andesite lava, volcanic breccia, boulder lava, tuff and lahar.	Reactioniation of NW - SE trend structure results the pathway for the intermediate magma rise to the surface and formed Quaternary volcano such Mt. Bukit Daun and Mt. Hulupalik					
				 Bukit Daun 2							
				 Bukit Daun 1							
				 Hulupalik 2	Andesite lava and andesite breccia						
				 Hulupalik 1							
				 Tiga							
Neogene			Regional Orogenic event  Increasing of subduction rate, uplift of Bukit Barisan range and further erosion  Sumatra Fault start faulting  Regressive in basin environment, shallow marine to transition.  Maximum transgressive	 Senayan	Andesit-basaltic volcanic breccia with epiclastic sediment intercalation	Unconformity - OROGENIC					
				 Lakitan							
				 	Dacitic epiclastic volcanic breccia		Major Strike-slip fault movement of Sumatra fault occur due to the pull-apart rifting on the Andaman Sea. (Kusnama et.al. 1992)				
								 			
				 	Intermediate intrusion Calc-alkaline volcanic activity Andesit-basaltic basaltic lava, andesite breccia, tuff, ad lapili (Tomh)						
								 			
				 	Tuffaceous sandstone (Toms)	Unconformity ?					
								 			
				Paleogene	Oligocene 23-34 Ma		Stabilized convergen rate of Indian - Australian plate.  Progressive deepening on the South Sumatera basin		Hulusimpang / Seblat	Volcanic breccia, welded tuff, tuff, lava, lava with intercalation of sandstone and shale	Unconformity ?
Eocene 34-56 Ma	Horst and Graben stage  Pre-rift stage		Kikim		Faulting of basement rocks creates Host & Graben (extensional) (Barber et.al. 2005)						
							Paleocene 56-66 Ma				
Cretaceous 66-145 Ma	Pre-rift stage  Final stage of stable craton	 	Shale, siltstone, with sandstone and chert intercalation (KJI)  Andesite to basaltic lava breccia tuff, epidotization, chloritisation, and propilitization (KJs)	Cretaceous and older rocks uplifted, folded and faulted with local metasomatism (McCarthy & Elders, 2014)							

### 3.4 Stratigraphic Model

The development of a 3D geological model demands a high geological interpretation level because of the limited constraints available from borehole data. However, the benefit is two-fold. First, ensuring the 3D model is plausible, makes geological sense, and is consistent with the available data, provides a quality-control step in geological interpretation. Second, once a 3D model is built, it enhances our ability to overlay quite different data types (e.g., hydrological data, potential field data) and then to modify key features according to new information. The development of a 3D geological model underpins the geothermal conceptual model.

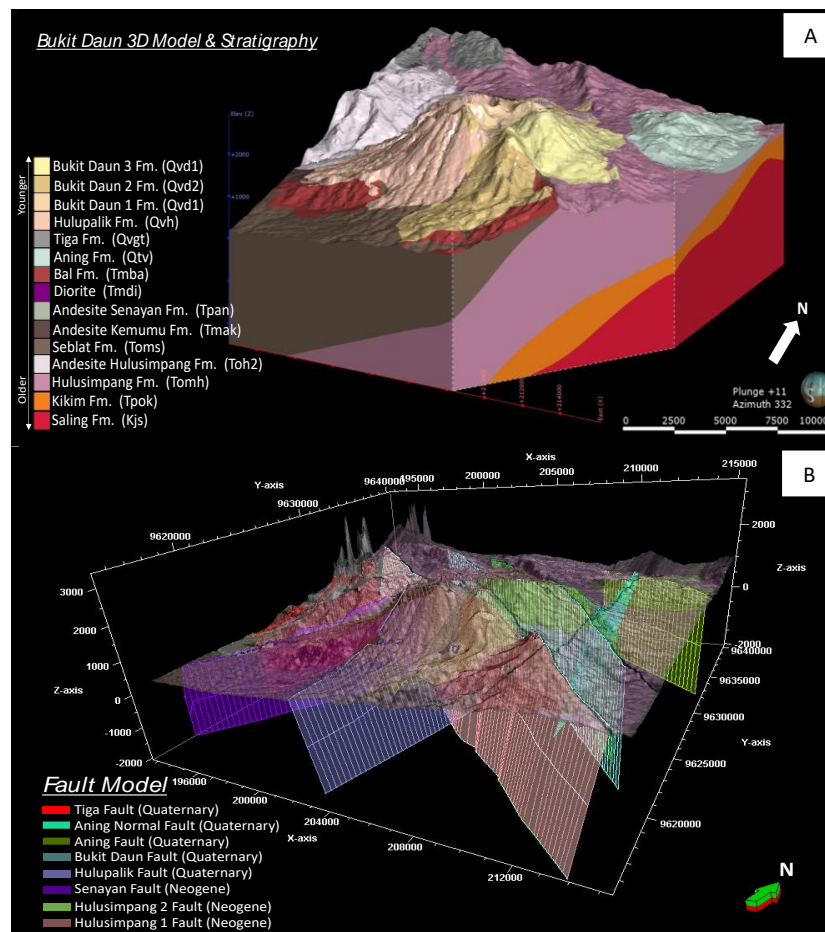
To build the model, the 2D cross-sections presented above were geo-referenced together with the topographic DEM and a 3D model volume (the model extends ten km<sup>2</sup>, to -2000 mRSL maximum depth and 3000 mRSL maximum elevations). In this study, model construction was undertaken using Leapfrog Geothermal and Petrel software.

Manual interpolation of formation contacts delineates the space between the cross-sections. The geometry of formation contacts was informed by evidence in the wells and also by regional geology. The cross-section tips reach the geological model extension. Formations mapped on the surface refer to the geological map, while the subsurface formations correspond with the borehole stratigraphic framework.



**Figure 9:** A) The geological map of the Bukit Daun field that we refined using the LiDAR and DEM images (key for the map is shown in Table 1). Red lines mark the position of cross-sections in Figures 9.B. The structural interpretation adapted from Ikhwan (2020). B) Cross-sections generated using surface and well data. Pre-Quaternary formations tilt and are likely part of a folds system with an NW-SE axis associated with the orogenic phase of compression. Quaternary volcanism sits unconformably on the eroded unconformity. Section locations are in Figure 9.A. The key for these sections in Table 1, where the geologic sequence is described.





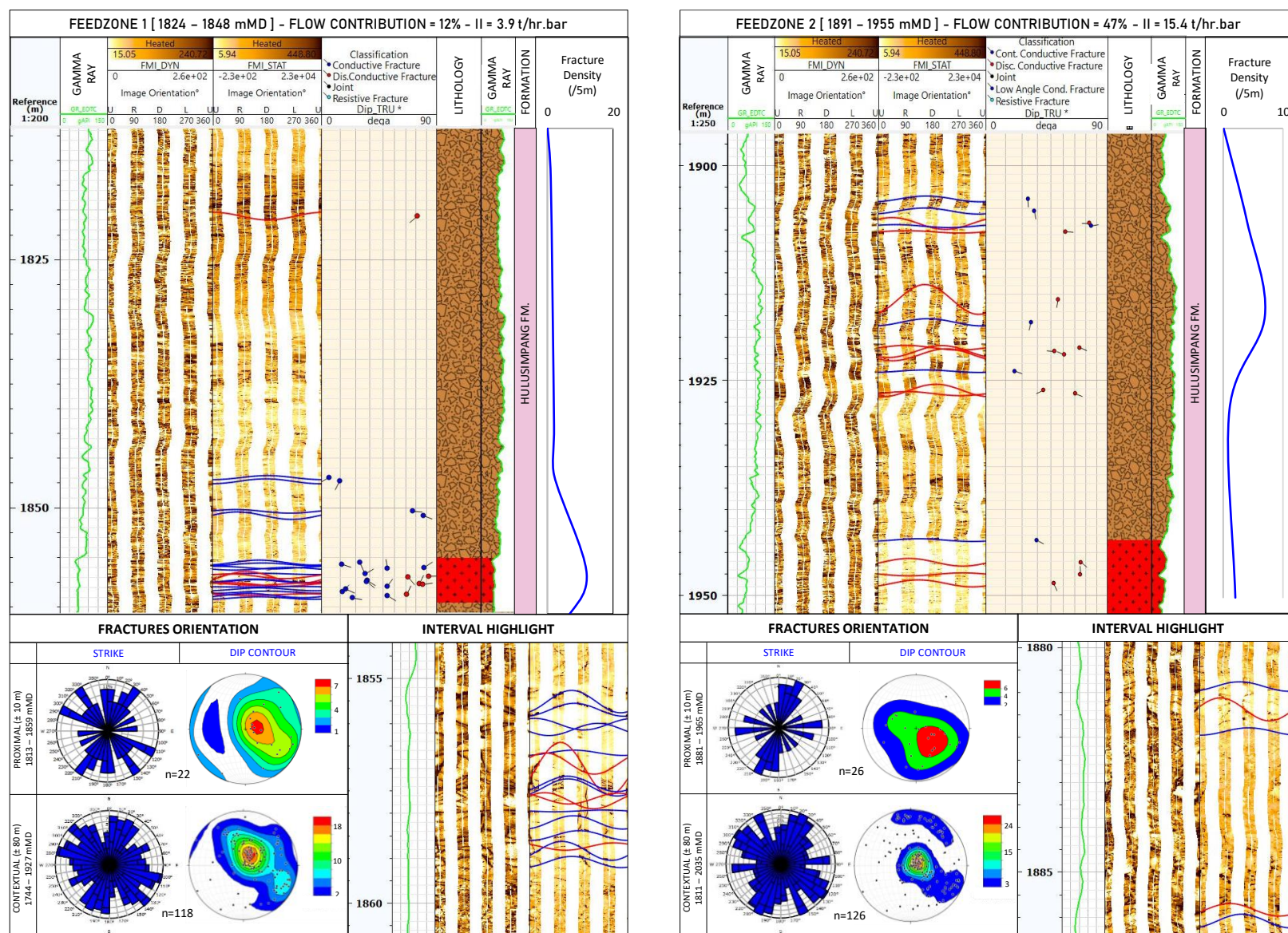
**Figure 10:** A) 3D stratigraphy model and B) Fault model of the Bukit Daun geothermal field. The geologic model is ten km<sup>2</sup> in the horizontal dimension and spans 2000 to 3000 mRSL in the vertical dimension. The stratigraphy model is sliced in a NE-SW direction to illustrate the geologic dip below the orogenic unconformity.

#### 4. STRATIGRAPHY INFLUENCE TO PERMEABILITY

Formation permeability also influences fluid flow, as demonstrated by the occurrence and character of high-flux feed zones in the volcanic breccia within this Hulusimpang formation conducted from Well-A test data (Ikhwan, 2020). Well-A is the hottest and has the highest injectivity (32.7 t/hr.bar). The mass flow is distributed on eight feedzones (Table 2). Figure 10 illustrates the lithology, fracture trends, and frequency interpreted from the micro-resistivity image logs. The purpose of these figures is to identify the correlation between the geological feature that is recorded in the image logs with feedzones derived from PTS. Figures contain three panels: (1) image log, to identify lithology and fractures, (2) fracture orientation, consisting of two intervals: proximal ( $\pm 10$  m above and below feedzone interval) to see the fracture orientation only in feedzone interval (local) and then to be compared with the contextual ( $\pm 80$  m above and below feedzone interval) to see the fracture orientations at reservoir scale, (3) highlight of image log, to see the certain geological features in more detail. In summary, there are two main permeability styles correlating to feedzones in Well-A, where the upper feedzones appear to be controlled by the matrix porosity from volcanic breccia (Feedzone 1 & 2), and these feedzones contribute most of the fluid flow. There is no clear trend in either the proximal or contextual fracture subsets, and there are few fractures compared with the deeper feedzones.

**Table 2:** Well-A feedzone contributions and lithological controls, with % contributions as inferred in this study (feedzone depths and total II provided by PGE, 2019). We divides the total II in the well into II for each feedzones, based on their % contribution in PTS, to make the particular II magnitude classification in the study area.

Feedzones	Measure Depth [mMD]	Elevation [mRSL]	Thickness [m]	Contribution [%]	II [t/hr.bar]	Control
Feed Zone 1	1824 - 1848	210 to 192	18	12	3.9	Breccia Dominated
Feed Zone 2	1891 - 1955	161 to 115	46	47	15.4	
Feed Zone 3	2423 - 2443	-302 to -317	15	1	0.3	
Feed Zone 4	2485 - 2514	-350 to -371	21	2	0.7	
Feed Zone 5	2540 - 2634	-391 to -461	70	<1	0.05	Fracture Dominated
Feed Zone 6	2745 - 2830	-490 to -556	66	11	3.6	
Feed Zone 7	2847 - 2883	-565 to -591	26	11	3.6	
Feed Zone 8	2896 - 2957	-600 to -644	44	16	5.2	
Total				100	32.7	



**Figure 10: Identification of well-scale permeability using the image log analysis shows a minimum fracture development in the productive intervals that lead the permeability interpretation to the productive volcanic breccia in Hulusimpang formation.**



## 5. CONCLUSION

The study area has a long history of volcanism from multiple sources, difficult to pinpoint due to burial by younger products. Considering the Quaternary volcanism only, at least four recent volcanoes around the study area could contribute to the stratigraphic sequence. Establishing a stratigraphic relationship in the study area is difficult because it is covered by a very dense tropical rainforest that obscures outcrops. The vast forest canopy also disguises structural evidence, especially for surface fault scarp identification.

The Bukit Daun field is a type of stratovolcano geothermal field that comprised an upflow area in the north flank of Mt. Bukit Daun (Well-A) and flows the hydrothermal fluid toward the north to the outflow zone in Well-C. The Bukit Daun geothermal field consists of Quaternary, Neogene, Paleogene, and Cretaceous formations where the Pre-Quaternary formations (e.g., Hulusimpang, Kikim, and Saling formation) act as the reservoir formations.

## ACKNOWLEDGEMENTS

Muhammad Ikhwan was funded by the MFAT of the New Zealand Postgraduate Scholarship program. We acknowledge PT. Pertamina Geothermal Energy provided data and permission to publish this paper. We thank Seequent (Leapfrog Geothermal) and Schlumberger (Techlog & Petrel) for the use of their software.

## REFERENCES

- Barber, A. J.; Crow, M. J.; Milsom, J. S. (2005). SUMATRA : Geology, Resources and Tectonic Evolution. Animal Genetics.
- Bellier, O., & Sébrier, M. (1994). Relationship between tectonism and volcanism along the Great Sumatran Fault Zone deduced by spot image analyses. Tectono-physics. [https://doi.org/10.1016/0040-1951\(94\)90242-9](https://doi.org/10.1016/0040-1951(94)90242-9)
- Bolli, H.M. and Saunders, J.B. 1985 Oligocene to Holocene low latitude planktonic foraminifera. In: H.M. Bolli. J.B. Saunders and K. Perch-Nielsen (eds), Plankton Stratigraphy. Cambridge Univ. Press, 155-262
- Darman, H., Sidi, F. H. (2000). An Outline of the Geology of Indonesia. Indonesian Association of Geologist-Jakarta.
- Gafoer S., Hermanto, & Amin, T. C. (1992) Geological Map of Indonesia, Bengkulu sheet, Scale 1:250,000, Geological Survey of Indonesia, Geological Research and Development Centre, Bandung.
- Hou, Z. J., & Wei, G. W. (2002). A new approach to edge detection. Pattern Recognition. [https://doi.org/10.1016/S0031-3203\(01\)00147-9](https://doi.org/10.1016/S0031-3203(01)00147-9)
- Ikhwan, M. (2020). Structural Framework of Bukit Daun Geothermal Field, Bengkulu: A Role of the Forearc Bengkulu Basin in Permeability. Proceedings the Digital Indonesia International Geothermal Conference & Exhibition, Jakarta, Indonesia.
- Ikhwan, M., Wallis, I. C., & Rowland, J. V. (2020). Geological Model and Permeability Framework of Bukit Daun Geothermal Field, Indonesia. Proceedings the 42<sup>nd</sup> New Zealand Geothermal Workshop, Waitangi, New Zealand.
- Kusnana, S. Andi Mangga., & D. Sukarna. (1992). Tertiary stratigraphy and tecton-ic evolution of southern Sumatra. Geological Research and Development Cen-ter, Bandung, Indonesia.
- McCarthy, A. J., & C. F. Elders, C. F. (1997). Cenozoic deformation in Sumatra: oblique subduction and the development of the Sumatran Fault System. Geological Society, London, Special Publications, 126, 355-363, 1.
- Moore, G. F., & Curray, J. R. (1980). Structure of the Sunda Trench lower slope off Sumatra from multichannel seismic reflection data. Marine Geophysical Research. <https://doi.org/10.1007/BF00369106>
- Postuma, J. (1971) Manual of Planktonic Foraminifera. Elsevier Publishing Co., Amsterdam, 420.
- PT. Pertamina Geothermal Energy Internal Report, Mt. Bukit Daun Geology, Geo-chemistry and Geophysics Survey Assessment, unpublished report for PT. Pertamina Geothermal Energy (2015).
- Sieh, K., & Natawidjaja, D. (2000). Neotectonics of the Sumatran fault, Indonesia. Journal of Geophysical Research: Solid Earth. <https://doi.org/10.1029/2000JB900120>